Khadem-Reza and Zare
Egypt J Neurol Psychiatry Neurosurg (2022) 58:135
https://doi.org/10.1186/s41983-022-00576-5

The Egyptian Journal of Neurology, Psychiatry and Neurosurgery

RESEARCH Open Access

Evaluation of brain structure abnormalities in children with autism spectrum disorder (ASD) using structural magnetic resonance imaging

Zahra Khandan Khadem-Reza and Hoda Zare*

Abstract

Background: Autism spectrum disorder (ASD) is a group of developmental disorders of the nervous system. Since the core cause of many of the symptoms of autism spectrum disorder is due to changes in the structure of the brain, the importance of examining the structural abnormalities of the brain in these disorder becomes apparent. The aim of this study is evaluation of brain structure abnormalities in children with autism spectrum disorder (ASD) using structural magnetic resonance imaging (sMRI). sMRI images of 26 autistic and 26 Healthy control subjects in the range of 5–10 years are selected from the ABIDE database. For a better assessment of structural abnormalities, the surface and volume features are extracted together from this images. Then, the extracted features from both groups were compared with the sample *t* test and the features with significant differences between the two groups were identified.

Results: The results of volume-based features indicate an increase in total brain volume and white matter and a change in white and gray matter volume in brain regions of Hammers atlas in the autism group. In addition, the results of surface-based features indicate an increase in mean and standard deviation of cerebral cortex thickness and changes in cerebral cortex thickness, sulcus depth, surface complexity and gyrification index in the brain regions of the Desikan–Killany cortical atlas.

Conclusions: Identifying structurally abnormal areas of the brain and examining their relationship to the clinical features of Autism Spectrum Disorder can pave the way for the correct and early detection of this disorder using structural magnetic resonance imaging. It is also possible to design treatment for autistic people based on the abnormal areas of the brain, and to see the effectiveness of the treatment using imaging.

Keywords: ASD, sMRI, ABIDE, Children, Brain

Background

The term autism is made up of two parts: autos, which means "self," and ism, which means "inclination" [1]. Autism Spectrum Disorder (ASD) is a group of developmental disorders of the nervous system. Its main manifestations consist of defects in social interactions, communication, repetitive behaviors and limited interests. Information from the US Department of Education shows that the incidence of autism increases by 10–17% each year [2]. Due to the rapid and progressive rise of ASD, a lot of research has been done on it recently. A major feature of ASD is the heterogeneity of its clinical features. A diversity of symptoms along with many psychological and physiological comorbidities may be present. Psychological comorbidities include attention–deficit hyperactivity disorder (ADHD), obsessive–compulsive disorder (OCD), anxiety, and intellectual disability [3]. There is a notable co-occurrence of ADHD with ASD, and the two conditions share many neurological and behavioral similarities. Physiological comorbidities of ASD include epilepsy, sleep disorders, and

*Correspondence: ZareH@mums.ac.ir

Department of Medical Physics, Faculty of Medicine, Mashhad University of Medical Sciences, Mashhad, Iran

gastrointestinal (GI) problems [4]. ASD are caused by genetic or environmental factors or a combination of these. ASD is considered a complex genetic disorder with high heritability. Epidemiological twin studies support the strong genetic component of ASD. Overall, the SFARI (Simons Foundation Autism Research Initiative) gene database, a database of autism candidate genes, lists about 1000 genes associated with ASD. Genes entered into the database are scored based on their strength of association with ASD risk. Despite the genetic heterogeneity, a recent review of the literature reveals that a number of these mutations converge on a common neurodevelopmental pathway involved in neurogenesis, axon guidance, and synapse formation. Non-genetic factors mediating ASD risk could include parental age, maternal nutritional and metabolic status, infection during pregnancy, prenatal stress, and exposure to certain toxins, heavy metals, or drugs [5]. For many years, brain development and function have been the focus of research in ASD. Experimental and postmortem studies have identified central nervous system (CNS) pathologies at gross morphological level and cellular level, for example, in neurons and glial cells. From these studies, it can be concluded that neuropathologies are evident in ASD. However, research in recent years on immune responses and gut–brain signaling have revealed that pathologies in ASD also exist outside the CNS [6].

ASD is diagnosed based on behavioral interests and repetitive behaviors [7]. These social impairments may be related to the interpretation of social signals: evidence from healthy individuals suggest that potentially threatening situations such as others' proximity can trigger a number of physiological responses that help regulate the distance between themselves and others during social interaction [8] and showing the critical role of social signal interpretation in social interaction [9]. Individuals with ASD have social impairments, potentially due to the lack of social signal interpretation and, therefore, resulting unable to interpret these signals to guide appropriate behaviors.

In the first step, identifying the clinical biomarkers of ASD using structural brain imaging can pave the way for recognizing the neurobiological causes of the disorder and the brain's areas affected by the disorder. In magnetic resonance imaging studies, there are generally two categories of features: volume-based and surface-based features. Different articles use one or a combination of both.

Several studies have been carried out to diagnose volumetric brain defects in people with autism. These studies reinforced the hypothesis that autistic patients had larger brain volumes than controls [10–15]. Several studies observed that the significant increased areas of gray and white matter volume in the autism group were the frontal, temporal and parietal lobes [16–19]. A more comprehensive study was conducted in 2016 by Haar and colleagues. This study showed an increase in ventricular volume, a decrease in the corpus collasom, and several cortical areas [20]. Several studies used Gyrification Index (GI) to distinguish between autistic and control groups. This index was higher in several regions in autistic than in the controls [21–24]. Several studies used the Sulcal depth parameter to analyze the shape anomalies of structural images. Abnormalities in the sum region were noticeable in the autistic group [25, 26]. In 2013, Ecker and colleagues. found, the thickness of the cerebral cortex was significantly larger in the frontal lobe of autistic subjects and the surface area in the orbitofrontal cortex and posterior cingulum in the autism group was lower than the control [27]. Sum studies examined cortical thickness changes and observed an increase of cortical thickness in several regions of the brain [20, 27–36]. The contradictory results reported in different studies have been due to differences in the imaging methods used, heterogeneity of the subjects and so on.

Since the core cause of many of the symptoms of autism spectrum disorder is due to changes in the structure of the brain, the importance of examining the structural abnormalities of the brain in these children becomes apparent. So far, few studies have been performed on structural abnormalities in the brains of autistic children. This study intended to investigate the images of structural magnetic resonance and also to detect structural abnormalities created in the brain attributable to autism spectrum disorder in children. In this study, to better evaluate, volume and surface features were employed simultaneously.

Methods

The steps performed in the study are shown in Fig. 1.

Subjects

IN this study, we used structural Magnetic Resonance images data from Autism Brain Imaging Data Exchange (ABIDE II). Because the aim of this study was to investigate the structural abnormalities of children's brains, we chose one data set acquired from NYU Langone Medical Center: Sample 1 (NYU) site. This data set consisted of 78 children's brain images. Due to the importance of early diagnosis of autism disorder for more effective treatment, the diagnosis of brain abnormalities at a younger age is more effective, and therefore, only children aged 5–10 years were examined in this study. Data from 26 autistic and 26 control subjects in the age range of 5–10 years were used in the present study. There was no significant difference in age and sex between autism

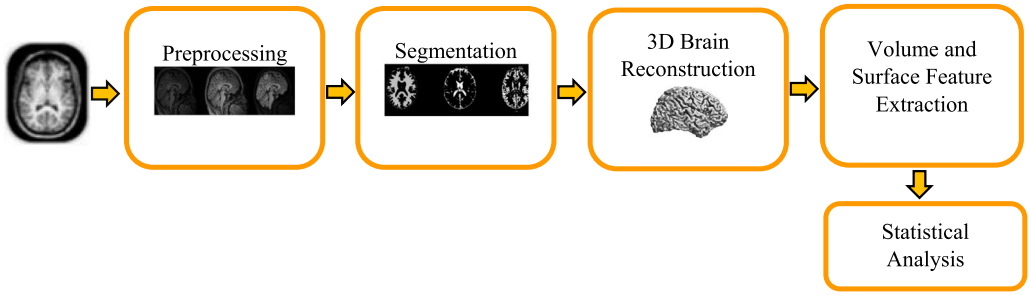

Fig. 1 Steps performed in the study

Table 1 Demographics for the participants

	ASD ($n=26$) Mean (STD)	HC ($n=26$) Mean (STD)	*P* value(*)
Age	7.12 (0.98)	7.48(1.39)	0.320
Sex	24M/2F	25M/1F	0.584
FIQ	100.64(26.85)	115.92(15.47)	0.016*
PIQ	100.23(19.77)	112.03(15.20)	0.020*
VIQ	99.96(15.69)	117.03(16.46)	< 0.001*
VABS Sum Scores	293.11(56.81)	332.68(50.33)	0.011*
SRS Total	75.07(17.27)	45.12(6.21)	< 0.001*

ASD Autism Spectrum Disorder, *HC* Healthy Controls, *M* Male, *STD* Standard Deviation, *F* Female, *FIQ* Full-Scale Intelligence Quotient, *PIQ* Performance Intelligence Quotient, *VIQ* Verbal Intelligence Quotient, *VABS* Vineland Adaptive Behavior Scales, *SRS* Social Responsiveness Scale; $P<0.05$ was considered statistically significant, *Statistically Significant

and healthy control groups. The demographic information of the participants is given in Table 1.

MRI acquisition

MRI scans were acquired from 3T scanners manufactured by Siemens with the Neuroimaging Informatics Technology Initiative (NIFTI) format with the following protocol: repetition time and echo time = 3.25 ms, flip angle = 7°, plane resolution = 1.3×1 mm, 1.3 mm slice thickness with 0.665 mm gap, 128 slices, 256×256 mm field of view, acquisition time = 8:07 min.

Preprocessing and segmentation

The CAT12 and SPM12 toolboxes in MATLAB software version R2019a have been used to process structural images of the brain. We performed the preprocessing steps using CAT12 toolboxes with the default setting, respectively. Briefly, all 3D T1-weighted MRI scans are normalized using an affine followed by non-linear registration, corrected for bias field inhomogeneities and then segmented into GM, WM, and CSF components [37]. For this procedure, we used the Diffeomorphic Anatomic Registration through Exponentiated Lie algebra algorithm (DARTEL) to normalize the segmented scans into a standard MNI space [38]. The pre-processing and segmentation steps are shown in Fig. 2. At the end of the image pre-processing and segmentation phase, there is a summarized QC index derived from CAT12, which can be used to represent the quality of the data. Furthermore, at least a visual inspection needs to be done. The pre-processing and segmentation steps are shown in Fig. 2.

3D brain reconstruction

Surface reconstruction steps are also performed using CAT12 toolbox in MATLAB R2019a software and include the following steps:

- Estimation of cerebral cortex thickness and central surface: we use a fully automated method that allows for the measurement of cortical thickness and reconstruction of the central surface in one step. It uses a tissue segmentation to estimate the white matter (WM) distance, then projects the local maxima (which is equal to the cortical thickness) to other gray matter voxels using a neighbor relationship described by the WM distance [39].
- Topological correction: topological correction is performed to repair topological defects using a method containing spherical harmonics that allows direct correction of defects on the brain surface mesh [40].

The reconstructed surface in the CAT12 toolbox is shown in Fig. 3.

Volume and surface feature extraction

Feature extraction is the process of extracting some unique and general data from an image. With the help of the designed algorithm, the features are extracted from the images, so that a feature vector is specified for each image. Extraction of sMRI features is done in two steps using the CAT12 toolbox:

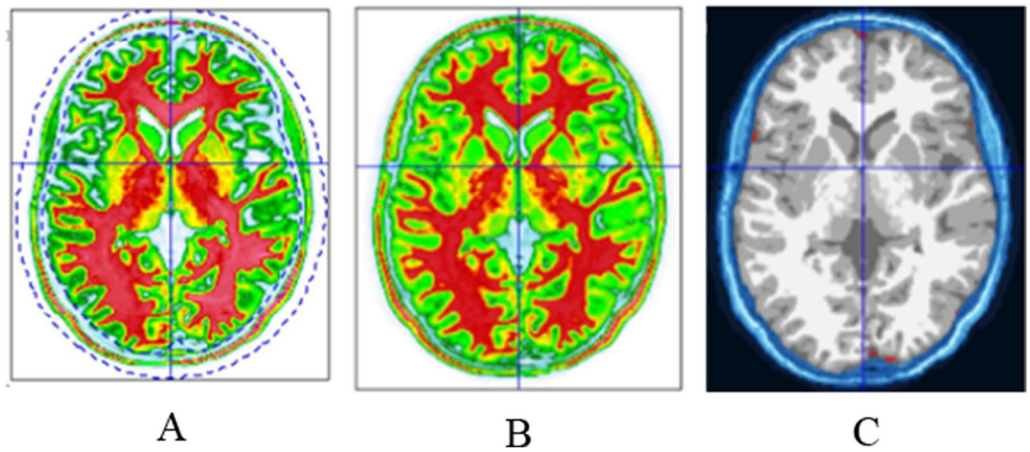

Fig. 2 Pre-processing steps in CAT12 toolbox. **A** Original image. **B** Image after intensity normalization. **C** Segmented image

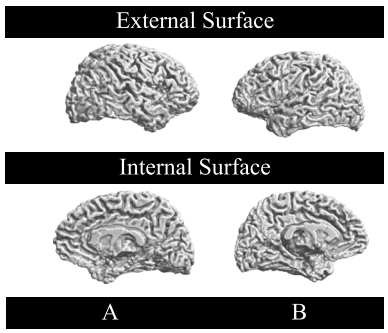

Fig. 3 Reconstructed surface by CAT12 toolbox. **A** Reconstruction of right hemisphere surface of the brain. **B** Reconstruction of left hemisphere surface of the brain

1) Volume-based features extraction: volume-based features include brain tissue volume measurements (white matter, gray matter and cerebrospinal fluid) and regional volume measurements of white matter and gray matter in 68 regions of the volume-based Hammer's Atlas.
2) Extraction of cortical-based features: cortical-based features include mean and standard deviation of cerebral cortex thickness and calculation of parameters of cerebral cortex thickness, cortical complexity, sulcus depth and GI in 68 regions of cortical-based Desikan–Killany Atlas. Cortical thickness in each region is defined as the Euclidean distance between the inner and outer layers of the cerebral cortex in that region. cortical complexity (CC) or fractal dimension (FD) provides a quantitative description of the structural complexity in the cerebral cortex. After extracting three-dimensional information from the cortex surface, FD is measured using the Box Counting algorithm. The three-dimensional surface is first covered using cubes of the same size. Then, the size of the cubes is changed and this is repeated. The fractal dimension is defined in three dimensions as logarithmic changes in the number of cubes divided by logarithmic changes in the size of the cubes. How to compute the fractal dimension is given in Eq. (1) [41]:

$$f_{3D} = -\frac{\Delta \log(\text{cube count})}{\Delta \log(\text{cube size})} \quad (1)$$

The sulcus is a groove in the cerebral cortex that usually surrounds a gyrus of the brain on both sides [42]. The human cerebral cortex has a complex morphological structure and is composed of folded or smooth cortical surfaces. These morphological features are referred to as cortical gyrification and are characterized by the GI. The GI is the ratio between the complete superficial contour ("the pial surface") and the outer contour of the cortical part of the cortex ("the outer smoothed surface"). How to compute this index is given in Eq. (2) [43]:

$$GI = \frac{\text{Length}(2D) \text{ or } \text{Surface}(3D) \text{ of pial surfaces}}{Length(2D) \text{ or surface}(3D) \text{ of Smoothed surfaces}} \quad (2)$$

Maps of surface parameters calculated by the CAT12 toolbox are prepared in Fig. 4.

The volume and surface features extracted from the structural magnetic resonance images are given in Table 2.

Statistical analysis

WE used the experimental sample *t* test and the Leven test to compare between groups for the continuous variable (age), and the chi-squared test for the qualitative variable (gender). After calculating the overall volumes of GM, WM, CSF and their sum (total intracranial

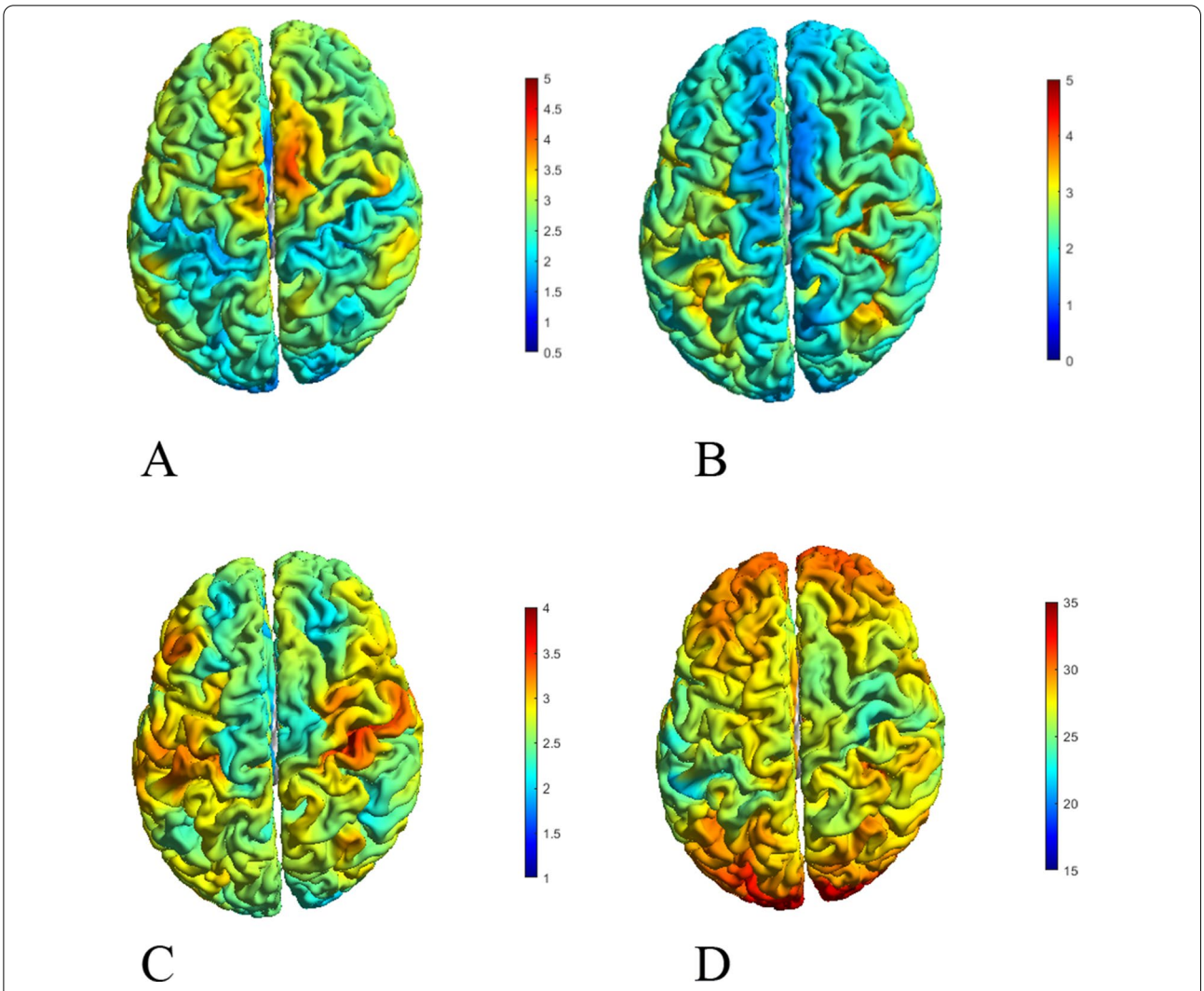

Fig. 4 Maps of surface parameters calculated by Toolbox CAT12. **A** Cortical thickness, **B** sulcus depth, **C** cortical complexity, **D** GI

volume; TIV), WM and GM per ROIs of hammers atlas and cortical thickness, sulcus depth, cortical complexity and GI per ROIs of DK atlas in two groups (independent variables), as estimated by the CAT12 toolbox, then, normality of these data was assessed using the Kolmogorov–Smirnov test. Then, for those variables in which the normality assumption was satisfied, independent sample *t* tests and Leven test was used. In other words, the nonparametric method (Mann–Whitney *U* test) and Leven test were used for non-normality values. The *P* value < 0.05 was considered statistically significant. The results were corrected with Bonferroni correction for multiple comparisons to be considered meaningful. All statistical analyses were performed using SPSS 26.0 software (SPSS Inc., Chicago, IL, USA).

Results

The findings of structural magnetic resonance image processing can be divided into volume-based and surface-based analysis.

Volume-based parameters

The statistically significant results of volumetric measurement of brain tissue are given in Table 3 and the statistically significant results of volumetric measurement of white matter and gray matter in the Hammers Atlas are also given in Tables 4 and 5, respectively.

Surface-based parameters

The statistical results of the mean and standard deviation of cortical thickness are shown in Table 6 and the

Table 2 Volume and surface features extracted from structural magnetic resonance images

Feature	Description
WMV T	White Matter Volume Total
GMV T	Gray Matter Volume Total
CSFV T	Cerebrospinal fluid Volume Total
TIV	Total Intracranial Volume
WMV	White Matter Volume per Hammers atlas
GMV	Gray Matter Volume per Hammers atlas
Mean CT	Mean Cortical Thickness per DK atlas
STD CT	Standard Deviation Cortical Thickness per DK atlas
CT	Cortical Thickness per DK atlas
CC	Cortical Complexity per DK atlas
SD	Sulcus Depth per DK atlas
GI	Gyrification Index per DK atlas

WMV T White Matter Volume Total, *GMV T* Gray Matter Volume Total, *CSF T* Cerebrospinal fluid Volume Total, *TIV* Total Intracranial Volume, *WMV* White Matter Volume, *GMV* Gray Matter Volume, *CT* Cortical Thickness, *STD* Standard Deviation, *CC* Cortical Thickness, *SD* Sulcus Depth, *GI* Gyrification Index

statistical results of cortical thickness, sulcus depth, GI and cortical complexity (fractal dimension) in DK atlas regions are also given in Tables 7, 8, 9 and 10, respectively.

Discussion

Autism spectrum disorder is associated with increased brain volume in childhood and decreased brain volume in adulthood [44]. Increased brain volume in autistic people compared to controls confirms the studies [10–19, 29]. Based on the statistical findings of the study presented in , the volume of white matter in the L and R amygdala region of the brain in the autism group shows a meaningful increase compared to the control. The amygdala is part of the limbic system of the brain and is associated with emotional and social behaviors [45], facial recognition [46], and cognitive function [47]. The increase in the volume of this area of the brain in the autistic group approves the research [13, 15, 48–51]. The volume of white matter in some areas located in the frontal and temporal lobes also has a considerable difference between two groups and is higher in the autism one, which confirms the studies [10, 17, 29, 52]. The frontal lobe in the brain is responsible for reasoning, planning, decision-making, and judgment, and generally controls social and cognitive behaviors [53]. The Temporal lobe is also involved in understanding language, and emotions, and is an area of sound and speech processing. Both lobes play a role in memory [54]. The volume of L and R putamen white matter, which is generally engaging in movement and learning [55], also is higher in the autism one that approves the studies [56–59]. The volume of white matter in the L and R thalamus and L precentral gyrus regions is notably lower in autism group. The thalamus is part of the limbic system of the brain that is the site of information amplification and processing. The precentral gyrus is known as the primary motor cortex which is responsible for voluntary movements [60]. The decrease in the volume of L and R thalamus confirmed by studies [61–63], however, is in contradiction with the study [64]. Decreased volume of L precentral gyrus has not been reported in any research. According to the statistical findings of the present analysis in Table 5, the volume of gray matter in the temporal lobe of the brain of autistic individuals compared to controls is meaningfully higher. In addition, considerable growth in the volume of the gray matter of R fusiform gyrus (FFG), L and R Pallidum and L corpus callosum in the autism group is observed. The social problems seen in ASD may be due in part to the dysfunction of FFG [65]. pallidum plays a role in the regulation of voluntary movements [66]. The corpus callosum is a group of high-density white matter fibers in the brain that facilitate communication between the hemispheres. The increase in gray matter volume of R fusiform gyrus, L and R pallidum and L corpus callosum in the autism group compared to controls is confirmed by researches [11, 14], [67, 68] and [69–73], respectively.

Neuroimaging research shows that human intellectual ability is related to the brain structure, including cortical thickness. Autism spectrum disorder is characterized by impaired cognition and social communication, and in addition to social disabilities [74]. Therefore, it is expected that the cortical thickness in autistic children is associated with abnormalities. Based on the statistical discoveries in Table 6, the mean and standard deviation of cortical thickness in the autism group, showing a notable increase which approves the studies [20, 27, 28, 30–36]. Furthermore, according to the statistical findings

Table 3 Statistical results of brain tissue volume measurement (significant differences)

	ASD		HC		Mean difference	*P* value
	Mean	STD	Mean	STD		
WMV T	484.26	48.06	440.88	30.56	48.38	< 0.001
TIV	1427.65	76.80	1378.61	75.68	49.03	0.025

ASD Autism Spectrum Disorder, *HC* Healthy Controls, *STD* Standard Deviation, *WMV T* White Matter Volume Total, *TIV* Total Intracranial Volume

Table 4 Statistical results of white matter volumetric measurements in Hammers Atlas regions (significant differences)

Brain region	ASD		HC		Mean Difference	*P* value
	Mean	STD	Mean	STD		
L amygdala	0.25	0.03	0.08	0.02	0.16	< 0.001
R amygdala	0.22	0.03	0.12	0.02	0.10	< 0.001
L anterior medial temporal lobe	2.59	0.23	1.56	0.26	1.02	< 0.001
R anterior medial temporal lobe	2.68	0.26	1.67	0.31	1.00	< 0.001
R superior temporal gyrus	6.25	0.61	5.38	0.57	0.87	< 0.001
L inferior middle temporal gyrus	6.47	0.68	5.54	0.63	0.93	< 0.001
R inferior middle temporal gyrus	6.72	0.64	5.69	0.64	1.03	< 0.001
L middle frontal gyrus	24.38	2.62	22.58	2.08	1.80	0.008
R middle frontal gyrus	24.86	2.71	22.73	2.06	1.13	0.002
L posterior temporal lobe	18.98	1.75	17.71	1.52	1.27	0.008
R posterior temporal lobe	19.26	1.73	17.98	1.74	1.28	0.010
L putamen	0.93	0.10	0.53	0.05	0.40	< 0.001
R putamen	1.07	0.10	0.63	0.07	0.43	< 0.001
L thalamus	2.47	0.40	2.68	0.36	− 0.21	< 0.001
R thalamus	2.44	0.29	2.68	0.38	− 0.23	< 0.001
L precentral gyrus	15.73	1.43	16.74	1.75	− 1.01	0.027
L orbitofrontal gyrus	6.71	0.61	5.95	0.56	0.6	< 0.001
R orbitofrontal gyrus	7.07	0.61	6.15	0.70	0.91	< 0.001
L inferior frontal gyrus	6.53	0.84	5.41	0.55	1.11	< 0.001
R inferior frontal gyrus	6.44	0.74	5.51	0.59	0.92	< 0.001

ASD Autism Spectrum Disorder, *HC* Healthy Controls, *STD* Standard Deviation, *L* Left, *R* Right

Table 5 Statistical results of gray matter in Hammers Atlas (significant differences)

Brain region	ASD		HC		Mean difference	*P* value
	Mean	SD	Mean	SD		
R superior temporal gyrus	10.48	0.82	9.82	0.77	0.65	0.005
R fusiform gyrus	4.22	0.36	3.58	0.48	0.63	< 0.001
L pallidum	0.71	0.08	0.65	0.11	0.06	0.026
R pallidum	0.76	0.08	0.71	0.11	0.05	0.049
L Corpus callosum	0.83	0.11	0.77	0.08	0.06	0.023
L lateral temporal ventricle	1.83	0.22	1.69	0.14	0.14	0.010

ASD Autism Spectrum Disorder, *HC* Healthy Controls, *STD* Standard Deviation, *L* Left, *R* Right

Table 6 Statistical results of mean and standard deviation of cortical thickness (significant differences)

Brain region	ASD		HC		Mean difference	*P* value
	Mean	STD	Mean	STD		
Mean CT	2.86	0.09	2.78	0.08	0.08	0.002
STD CT	0.95	0.05	0.88	0.05	0.10	< 0.001

ASD Autism Spectrum Disorder, *HC* Healthy Controls, *STD* Standard Deviation, *Mean CT* Mean Cortical Thickness per DK atlas, *STD CT* Standard Deviation Cortical Thickness per DK atlas

in Table 7, the cortical thickness in the L and R cuneus, R lingual, R paracentral, L parsopercularis and R superior temporal areas in the autism group has a considerable increase. cuneus and lingual are parts of the brain located in the occipital lobe and are engaged in visual processing [75, 76]. The paracentral controls the sensory and motor nerves of the lower extremity [77]. Pars operculris is a part of the inferior frontal gyrus located in the Broca area

Table 7 Statistical results of cortical thickness parameter in DK atlas regions (significant differences)

Brain region	ASD		HC		Mean difference	*P* value
	Mean	STD	Mean	STD		
L cuneus	2.40	0.12	2.19	0.02	0.21	< 0.001
R cuneus	2.40	0.12	2.21	0.02	0.18	< 0.001
R lingual	2.41	0.06	2.35	0.13	0.06	0.049
L parahippocampal	2.35	0.23	2.46	0.08	− 0.11	0.027
R parahippocampal	2.39	0.28	2.55	0.14	− 0.015	0.015
R paracentral	2.88	0.09	2.77	0.02	0.12	< 0.001
L parsopercularis	2.82	0.05	2.75	0.14	0.06	0.043
R superior temporal	3.06	0.06	2.98	0.19	0.08	0.039

ASD Autism Spectrum Disorder, *HC* Healthy Controls, *STD* Standard Deviation, *L* Left, *R* Right

Table 8 Statistical results of Sulcus depth parameter in Atlas DK areas (significant differences)

Brain region	ASD		HC		Mean difference	*P* value
	Mean	STD	Mean	STD		
L bankssts	3.53	0.29	3.38	0.18	0.15	0.032
L parsopercularis	3.87	0.29	3.72	0.10	0.15	0.015
L parstriangularis	3.49	0.36	3.30	0.13	0.18	0.015
R rostral anterior cingulate	2.48	0.11	2.53	0.03	− 0.05	0.041
L superior temporal	2.69	0.36	2.54	0.12	0.15	0.048
L temporal pole	2.89	0.39	2.71	0.12	0.17	0.033
R temporal pole	3.05	0.34	2.88	0.13	0.17	0.023
L insula	5.54	0.32	5.41	0.10	0.13	0.049

ASD Autism Spectrum Disorder, *HC* Healthy Controls, *STD* Standard Deviation, *L* Left, *R* Right

Table 9 Statistical results of gyrification index parameter in DK Atlas regions (significant differences)

Brain region	ASD		HC		Mean difference	*P* value
	Mean	STD	Mean	STD		
L entorhinal	27.40	2.81	29.12	1.56	− 1.71	0.009
R inferior parietal	34.50	2.12	31.47	0.41	3.02	< 0.001
L inferior temporal	27.66	0.84	27.08	0.59	0.5720	0.007
L lateral occipital	33.35	0.58	30.89	0.17	2.46	< 0.001
R lateral occipital	33.42	0.80	30.66	0.14	2.75	< 0.001
R parstriangularis	27.82	1.52	27.19	0.54	0.63	0.049
L posterior cingulate	29.47	0.82	29.05	0.30	0.42	0.018
L precuneus	29.92	0.94	27.92	0.16	2.00	< 0.001
R superior parietal	30.67	1.08	28.88	0.31	1.79	< 0.001
L fronta pole	34.23	1.52	32.14	0.30	2.09	< 0.001

ASD Autism Spectrum Disorder, *HC* Healthy Controls, *STD* Standard Deviation, *L* Left, *R* Right

of the brain [78]. The Broca area in the brain is related to speech production and processing [79]. Since speech disorder is one of the main features of ASD, this area is one of the main parts that encounter abnormalities in autism spectrum disorder [80, 81]. The superior temporal is part of the temporal lobe and contains the auditory cortex, which is responsible of processing sounds. It also includes the Wernicke area of the brain, which is the main part for understanding language. This area also plays a vital role in social cognition and impairment of this part is one of the main features of ASD [82, 83]. Increased cerebral cortical thickness in L and R cuneus, R lingual, R paracentral areas has not been reported in any study. Increased cortical thickness of the L parsopercularis and

Table 10 Statistical results of surface complexity parameter (fractal dimension) in DK Atlas regions (significant differences)

Brain region	ASD		HC		Mean difference	*P* value
	Mean	STD	Mean	STD		
R bankssts	2.31	0.48	2.58	0.14	− 0.27	0.009
R caudate anterior cingulate	1.90	0.44	2.23	0.15	− 0.31	0.001
R caudate middle frontal	2.35	0.45	2.67	0.15	− 0.32	0.001
R cuneus	2.05	0.38	2.26	0.08	− 0.20	0.011
R entorhinal	2.09	0.45	2.37	0.14	− 0.28	0.003
R fusiform	2.03	0.45	2.34	0.16	− 0.30	0.003
R inferior parietal	2.19	0.42	2.47	0.14	− 0.28	0.003
R inferior temporal	1.91	0.40	2.15	0.10	− 0.23	0.006
L isthmus cingulate	2.00	0.14	2.06	0.05	− 0.06	0.044
R isthmus cingulate	1.50	0.48	1.85	0.20	− 0.34	0.002
R lateral occipital	1.88	0.41	2.15	0.13	− 0.27	0.003
R lateral orbitofrontal	1.84	0.42	2.13	0.13	− 0.28	0.002
R lingual	2.09	0.49	2.39	0.15	− 0.29	0.006
L medial orbitofrontal	2.55	0.16	2.64	0.05	− 0.08	0.022
R medial orbitofrontal	2.07	0.48	2.38	0.15	− 0.30	0.003
R middle temporal	2.03	0.12	2.33	0.16	− 0.29	0.003
L parahippocampal	2.59	0.11	2.64	0.03	− 0.04	0.047
R parahippocampal	1.99	0.57	2.30	0.18	− 0.30	0.014
R paracentral	2.05	0.43	2.32	0.14	− 0.27	0.004
R parsopercularis	2.31	0.50	2.62	0.17	− 0.30	0.005
L parsorbitalis	2.96	0.20	3.05	0.10	− 0.09	0.034
R parsorbitalis	2.30	0.50	2.63	0.18	− 0.32	0.004
L parstriangularis	2.66	0.12	2.73	0.06	− 0.07	0.011
R parstriangularis	2.25	0.44	2.50	0.12	− 0.24	0.008
R pericalcarine	1.79	0.42	2.10	0.16	− 0.31	0.001
R postcentral	2.30	0.39	2.60	0.16	− 0.29	0.001
R posterior cingulate	1.94	0.45	2.23	0.15	− 0.28	0.003
R precentral	2.25	0.43	2.54	0.15	− 0.29	0.002
R precuneus	2.05	0.45	2.33	0.14	− 0.27	0.004
R rostral anterior cingulate	1.49	0.36	1.71	0.08	− 0.21	0.006
R rostral middle frontal	1.99	0.44	2.27	0.14	− 0.28	0.014
R superior frontal	1.81	0.40	2.07	0.12	− 0.25	0.003
R superior parietal	2.11	0.40	2.36	0.12	− 0.25	0.004
R superior temporal	2.21	0.43	2.50	0.15	− 0.29	0.002
R supramarginal	2.07	0.40	2.32	0.12	− 0.24	0.004
R frontal pole	2.23	0.46	2.50	0.13	− 0.27	0.006
R temporal pole	2.02	0.40	2.28	0.12	− 0.25	0.003
R transverse temporal	1.62	0.45	1.94	0.17	− 0.31	0.002
R insula	1.81	0.38	2.01	0.08	− 0.02	0.012

ASD Autism Spectrum Disorder, *HC* Healthy Controls, *STD* Standard Deviation, *L* Left, *R* Right

R superior temporal also confirms studies [84, 85] and [30], respectively. In addition, the cortical thickness of L and R parahippocampal areas in the autism group was notably decreased. The parahippocampal is a part of the limbic system of the brain that plays an important role in encoding and retrieving memory [86]. This finding of the current research confirms the study [87]. Based on the statistical findings of the present study in Table 8, the Sulcus depth of the cerebellum of L bankssts, L parsopercularis, L parstriangularis, L superior temporal, L and R temporal pole and L insula in the autism group shows a substantial increase [25, 26, 88, 89]. In ASD, the presence of anomalies in bankssts is the root of the impairment in the social activities [90]. The parstriangularis, like

the parsopercularis, is part of the inferior frontal gyrus located in the Broca area of the brain [85]. Insula also participates in understanding consciousness and social emotions [86, 87]. The sulcus depth of the rostral anterior cingulate in the autism group showed a significant decrease compared to the control group, which has not been reported in any study. According to the statistical data of Table 9, the GI of the number of frontal and parietal lobe brain regions in the autism group has increased considerably. Furthermore, this index has increased in L and R lateral occipital, R parstriangularis, L posterior cingulate, L precuneus, in the autism group compared to the control group. This finding of the present analysis confirms the studies [21–24, 91–94]. On the other hand, this index in the L entorhinal brain area in the autism group is substantially reduced compared to the control group. Posterior cingulate is involved in memory and emotion [95, 96] and researches have revealed that abnormality of this region is one of the main aspects of ASD [97]. The precuneus is a region of the brain that participated in a variety of complex functions, including recall and memory, the integration of information about the environment, mental imagery strategies, memory retrieval, and emotional responses [98]. The entorhinal is located in the middle of the temporal lobe and acts as an extensive network in memory and time perception [99]. According to the statistical findings of Table 10, the cortical complexity parameter in all areas of the right hemisphere of the autism group compared to the control group has meaningfully decreased. In addition, there is an important difference between the two groups in the some regions of the brain located in the left hemisphere. So far, no study has been performed to calculate the surface cortical complexity parameter in the DK atlas regions. However, according to the clinical characteristics of autism spectrum disorder and abnormal areas, the findings of the present study can be correctly understood.

Regions in the frontal and parietal cortices, are involved in a number of cognitive operations, including planning, working memory, impulse control, inhibition, and set-shifting. These cognitive domains are often referred to under the umbrella term of "executive functions," which broadly refers to the set of processes that are employed when an individual is involved in a goal-directed activity. Damage to the frontal cortex, which is considered the "seat" of executive functioning, interrupts the ability of individuals to complete many goal-directed tasks and has been shown to result in the emergence of perseverative and repetitive behaviors, insistence for sameness, and impulsivity, all of which are clinical manifestations of autism spectrum disorders [100]. Prefrontal cortex is one region of the emotion processing network. The prefrontal cortex is like a control center, helping to guide our actions, and therefore, this area is also involved during emotion regulation. In the recent years, growing attention has paid to the involvement of cerebellar and striatal structures in ASD. In the recent years, growing attention has paid to the involvement of cerebellar and striatal structures in ASD. The cerebellum is involved in both motor and social impairments reported in ASD. Clumsiness and deficits in motor coordination and manual dexterity, abnormal balance gait and posture are all dependent on the cerebellar function and are affected in ASD. These deficits can be detected even in the first months of life, with affected babies exhibiting difficulties positioning their body when carried, hypotonia and uncoordinated movements. The basal ganglia are a group of subcortical nuclei involved primarily in motor skills. The term "Basal Ganglia" refers to the striatum and the globus pallidus, while the substantia nigra (mesencephalon), the subthalamic nuclei (diencephalon) and the pons are related nuclei. Basal ganglia network is shown to be deeply affected in ASD models. In the early 2000s, John Rubenstein and Michael Merzenich formulated the excitation/inhibition (E/I) imbalance hypothesis of ASD, suggesting that the physiopathology of ASD and their related comorbidities may reflect a disturbance in such a balance. Even though their work focused only on the cortical networks, it may be easily extended to striatal networks, as the striatum receives major excitatory inputs from cortices areas and major inhibitory inputs from the local interneurons network [101].

Autism diagnostic methods are currently based on clinical observations, but these methods have many errors. The use of diagnostic methods in parallel with imaging methods can have a great impact on the design of treatment processes for these patients. There are various methods for treating autism, including speech therapy, occupational therapy, music therapy, game therapy, behavioral therapy. A combination of these treatment methods can reduce the symptoms of this disease and control it. Since autism is a spectrum disorder and the severity of symptoms is not the same in all patients, a fixed treatment method cannot be used for all patients. In general, the method of structural imaging of the brain and the examination of structural abnormalities of the brain of autistic people helps to design personal treatment for each patient and to choose an effective treatment method. Using the method of this study, it is possible to evaluate the effect of therapeutic interventions on the patient's recovery process, and if the desired result is not achieved, another treatment method substituted. With brain structural imaging, the abnormal areas of the brain are identified, and based on the abnormal areas of each person's brain, along with clinical observations, personalized treatment is designed. In addition,

after a period of speech therapy, neuroimaging can be done again, and by comparing the results of two imaging sessions, the treatment process can be evaluated and the improvement of structural abnormalities in these areas can be observed, which indicates the progress of the treatment.

Conclusions

This study aimed to investigate and identify structurally abnormality areas of the brain in autism spectrum disorder using structural magnetic resonance imaging. In examining the brain volume using sMRI, simultaneous volume changes of gray matter and cerebral white matter were observed in the autism group. These volume changes are in the form of an increase in the total volume of the brain and white matter of the brain and changing in the volume of white and gray matter in the identified areas of the Hammers volume in the autism group. Examining the brain surface using sMRI also showed abnormalities in the parameters of cerebral cortex thickness, sulcus depth, surface complexity and GI in the autism group. These changes are increasing the mean and standard deviation of the cerebral cortex thickness and changing the mentioned parameters in the specified areas of the DK atlas in the autism group. Changes in the brain structure due to ASD are often related to the clinical features of autism spectrum disorder, such as the Broca and Wernicke areas, which are involved in speech production and speech comprehension. Identifying structurally abnormality areas of the brain and examining their relationship to the clinical features of ASD can pave the way for the correct and early detection of this disorder using structural magnetic resonance imaging. It is also possible to design treatment for autistic people based on the abnormal areas of the brain, and to see the effectiveness of the treatment using imaging.

The impossibility of collecting imaging and clinical information led to the use of ABIDE data. As well as the lack of imaging and clinical data of infants in both autism and control groups, caused the use of subjects in the age range of 5–10 years. In addition, ASD is an extremely heterogenous disorder, were any of the selected patients suffered from associated low IQ, delayed speech, epilepsy or any other forms of associated diseases. Those comorbidities can affect both the volume and surface of brain, which could affect specifity of the diagnosis. Since there is no information about autism associated diseases in selected patients, this problem is one of the limitations of the present study. It is suggested that the study be performed for more detailed research with a higher amount of data. In addition, it can be organized by information from patients who suffer from autism and the control group with younger age. Other methods of analyzing structural magnetic resonance imaging should also be observed. Studies with similar data should be done using other software. The present analysis has focused on the structure of the brain. In future researches, in addition to structural images of the brain, other brain imaging modalities such as fMRI and DTI can be used. Due to the dependence of brain structure on age, studies can be performed in different age groups to identify the effect of age on changes in brain structure due to autism spectrum disorder.

Abbreviations

ASD: Autism spectrum disorder; SMRI: Structural magnetic resonance imaging; ABIDE: Autism brain imaging data exchange; NIFT: Neuroimaging informatics technology initiative; GI: Gyrification index; HC: Healthy controls; M: Male; F: Female; FIQ: Full-scale intelligence quotient; PIQ: Performance intelligence quotient; VIQ: Verbal intelligence quotient; VABS: Vineland adaptive behavior scales; SRS: Social responsiveness scale; CAT: Computational anatomy toolbox; SPM: Statistical parametric mapping; DARTEL: Diffeomorphic Anatomic Registration Through Exponentiated Lie algebra algorithm; MNI: Montreal Neurological Institute; GM: Gray matter; WM: White matter; CSF: Cerebrospinal fluid; CC: Cortical complexity; CT: Cortical thickness; STD: Standard deviation; FD: Fractal dimension; ROI: Region of interest; DK: Desikan–Killiany; L: Left; R: Right; FFG: Fusiform gyrus; FMRI: Functional magnetic resonance imaging; DTI: Diffusion tensor imaging.

Acknowledgements

This paper was extracted from a MS.c thesis of Medical Physics. The authors would like to thank the Research Deputy of MUMS for financial support of this project, numbered (980858). Ethics code: IR.MUMS.MEDICAL.REC.1398.717)

Author contributions

HZ contributed as a research assistant as well as a technical advisor. ZK was a major contributor to image analyzing and writing the manuscript. All authors read and approved the final manuscript.

Funding

The Research Deputy of Mashhad University of Medical Sciences financially supported this research in Terms of M.Sc. dissertation.

Availability of data and materials

The data sets used and/or analyzed during the current study are available from the corresponding author on Reasonable request.

Declarations

Ethics approval and consent to participate

In this study, patients do not participate directly in the design and only images of people with autism and the control group that have already been evaluated are extracted from the ABIDE database (https://fcon_1000.projects.nitrc.org/indi/abide/abide_I.html).

Consent for publication

Not applicable.

Competing interests

The authors declare that they have no competing interests.

Received: 26 April 2022 Accepted: 26 October 2022
Published online: 18 November 2022

References

1. Harper D. Online etymological dictionary. Retrieved April 2, 2008.
2. Edition F. Diagnostic and statistical manual of mental disorders. Am Psychiatric Assoc. 2013;21(21):591–643.

3. Brookman-Frazee L, Stadnick N, Chlebowski C, Baker-Ericzén M, Ganger W. Characterizing psychiatric comorbidity in children with autism spectrum disorder receiving publicly funded mental health services. Autism. 2018;22(8):938–52.
4. Abuaish S, Al-Otaibi NM, Abujamel TS, Alzahrani SA, Alotaibi SM, AlShawakir YA, Aabed K, El-Ansary A. Fecal transplant and Bifidobacterium treatments modulate gut Clostridium bacteria and rescue social impairment and hippocampal BDNF expression in a rodent model of autism. Brain Sci. 2021;11(8):1038.
5. Tanaka M, Tóth F, Polyák H, Szabó Á, Mándi Y, Vécsei L. Immune influencers in action: metabolites and enzymes of the tryptophan-kynurenine metabolic pathway. Biomedicines. 2021;9(7):734.
6. Sauer AK, Stanton J, Hans S, Grabrucker A. Autism spectrum disorders: etiology and pathology. Exon Publications; 2021. p. 1–5.
7. Roehr B. American psychiatric association explains DSM-5. BMJ. 2013;6:346.
8. Candini M, Battaglia S, Benassi M, di Pellegrino G, Frassinetti F. The physiological correlates of interpersonal space. Sci Rep. 2021;11(1):1–8.
9. Ellena G, Battaglia S, Làdavas E. The spatial effect of fearful faces in the autonomic response. Exp Brain Res. 2020;238(9):2009–18.
10. Courchesne E, Karns C, Davis H, Ziccardi R, Carper R, Tigue Z, et al. Unusual brain growth patterns in early life in patients with autistic disorder: an MRI study. Neurology. 2001;57(2):245–54.
11. Waiter GD, Williams JH, Murray AD, Gilchrist A, Perrett DI, Whiten A. A voxel-based investigation of brain structure in male adolescents with autistic spectrum disorder. Neuroimage. 2004;22(2):619–25.
12. Hazlett HC, Poe M, Gerig G, Smith RG, Provenzale J, Ross A, et al. Magnetic resonance imaging and head circumference study of brain size in autism: birth through age 2 years. Arch Gen Psychiatry. 2005;62(12):1366–76.
13. Katuwal GJ, Baum SA, Cahill ND, Dougherty CC, Evans E, Evans DW, et al. Inter-method discrepancies in brain volume estimation may drive inconsistent findings in autism. Front Neurosci. 2016;10:439.
14. Salmond CH, Vargha-Khadem F, Gadian DG, de Haan M, Baldeweg T. Heterogeneity in the patterns of neural abnormality in autistic spectrum disorders: evidence from ERP and MRI. Cortex. 2007;43(6):686–99.
15. Bellani M, Calderoni S, Muratori F, Brambilla P. Brain anatomy of autism spectrum disorders II. Focus on amygdala. Epidemiol Psychiatr Sci. 2013;22(4):309–12.
16. Herbert MR, Ziegler DA, Makris N, Filipek PA, Kemper TL, Normandin JJ, et al. Localization of white matter volume increase in autism and developmental language disorder. Ann Neurol. 2004;55(4):530–40.
17. Carper RA, Courchesne E. Localized enlargement of the frontal cortex in early autism. Biol Psychiat. 2005;57(2):126–33.
18. Hardan AY, Muddasani S, Vemulapalli M, Keshavan MS, Minshew NJ. An MRI study of increased cortical thickness in autism. Am J Psychiatry. 2006;163(7):1290–2.
19. Toal F, Daly E, Page L, Deeley Q, Hallahan B, Bloemen O, et al. Clinical and anatomical heterogeneity in autistic spectrum disorder: a structural MRI study. Psychol Med. 2010;40(7):1171.
20. Haar S, Berman S, Behrmann M, Dinstein I. Anatomical abnormalities in autism? Cereb Cortex. 2016;26(4):1440–52.
21. Hardan AY, Jou RJ, Keshavan MS, Varma R, Minshew NJ. Increased frontal cortical folding in autism: a preliminary MRI study. Psychiatry Research: Neuroimaging. 2004;131(3):263.
22. Wallace GL, Robustelli B, Dankner N, Kenworthy L, Giedd JN, Martin A. Increased gyrification, but comparable surface area in adolescents with autism spectrum disorders. Brain. 2013;136(6):1956–67.
23. Awate SP, Win L, Yushkevich P, Schultz RT, Gee JC, editors. 3D cerebral cortical morphometry in autism: increased folding in children and adolescents in frontal, parietal, and temporal lobes. International Conference on Medical Image Computing and Computer-Assisted Intervention; Springer. 2008
24. Ecker C, Andrews D, Dell'Acqua F, Daly E, Murphy C, Catani M, et al. Relationship between cortical gyrification, white matter connectivity, and autism spectrum disorder. Cereb Cortex. 2016;26(7):3297–309.
25. Nordahl CW, Dierker D, Mostafavi I, Schumann CM, Rivera SM, Amaral DG, et al. Cortical folding abnormalities in autism revealed by surface-based morphometry. J Neurosci. 2007;27(43):11725–35.
26. Dierker DL, Feczko E, Pruett JR Jr, Petersen SE, Schlaggar BL, Constantino JN, et al. Analysis of cortical shape in children with simplex autism. Cereb Cortex. 2015;25(4):1042–51.
27. Ecker C, Ginestet C, Feng Y, Johnston P, Lombardo MV, Lai M-C, et al. Brain surface anatomy in adults with autism: the relationship between surface area, cortical thickness, and autistic symptoms. JAMA Psychiat. 2013;70(1):59–70.
28. Zielinski BA, Prigge MB, Nielsen JA, Froehlich AL, Abildskov TJ, Anderson JS, et al. Longitudinal changes in cortical thickness in autism and typical development. Brain. 2014;137(6):1799–812.
29. Pagnozzi AM, Conti E, Calderoni S, Fripp J, Rose SE. A systematic review of structural MRI biomarkers in autism spectrum disorder: a machine learning perspective. Int J Dev Neurosci. 2018;71:68–82.
30. Hyde KL, Samson F, Evans AC, Mottron L. Neuroanatomical differences in brain areas implicated in perceptual and other core features of autism revealed by cortical thickness analysis and voxel-based morphometry. Hum Brain Mapp. 2010;31(4):556–66.
31. Patriquin MA, DeRamus T, Libero LE, Laird A, Kana RK. Neuroanatomical and neurofunctional markers of social cognition in autism spectrum disorder. Hum Brain Mapp. 2016;37(11):3957–78.
32. Sharda M, Foster NE, Tryfon A, Doyle-Thomas KA, Ouimet T, Anagnostou E, et al. Language ability predicts cortical structure and covariance in boys with autism spectrum disorder. Cereb Cortex. 2017;27(3):1849–62.
33. Sharda M, Khundrakpam BS, Evans AC, Singh NC. Disruption of structural covariance networks for language in autism is modulated by verbal ability. Brain Struct Funct. 2016;221(2):1017–32.
34. Valk SL, Di Martino A, Milham MP, Bernhardt BC. Multicenter mapping of structural network alterations in autism. Hum Brain Mapp. 2015;36(6):2364–73.
35. Van Rooij D, Anagnostou E, Arango C, Auzias G, Behrmann M, Busatto GF, et al. Cortical and subcortical brain morphometry differences between patients with autism spectrum disorder and healthy individuals across the lifespan: results from the ENIGMA ASD Working Group. Am J Psychiatry. 2018;175(4):359–69.
36. Andrews DS, Avino TA, Gudbrandsen M, Daly E, Marquand A, Murphy CM, et al. In vivo evidence of reduced integrity of the gray–white matter boundary in autism spectrum disorder. Cereb Cortex. 2017;27(2):877–87.
37. Ashburner J, Friston KJ. Unified segmentation. Neuroimage. 2005;26(3):839–51. https://doi.org/10.1016/j.neuroimage.2005.02.018.
38. Klein A, Andersson J, Ardekani BA, Ashburner J, Avants B, Chiang MC, et al. Evaluation of 14 nonlinear deformation algorithms applied to human brain MRI registration. Neuroimage. 2009;46(3):786–802. https://doi.org/10.1016/j.neuroimage.2008.12.037.
39. Dahnke R, Yotter RA, Gaser C. Cortical thickness and central surface estimation. Neuroimage. 2013;65:336–48.
40. Yotter RA, Dahnke R, Thompson PM, Gaser C. Topological correction of brain surface meshes using spherical harmonics. Hum Brain Mapp. 2011;32(7):1109–24.
41. Lu H. Quantifying age-associated cortical complexity of left dorsolateral prefrontal cortex with multiscale measurements. J Alzheimers Dis. (Preprint):1–12.
42. Hopkins WD, Meguerditchian A, Coulon O, Misiura M, Pope S, Mareno MC, et al. Motor skill for tool-use is associated with asymmetries in Broca's area and the motor hand area of the precentral gyrus in chimpanzees (Pan troglodytes). Behav Brain Res. 2017;318:71–81.
43. Mietchen D, Gaser C. Computational morphometry for detecting changes in brain structure due to development, aging, learning, disease and evolution. Front Neuroinform. 2009;3:25.
44. Courchesne E, Campbell K, Solso S. Brain growth across the life span in autism: age-specific changes in anatomical pathology. Brain Res. 2011;1380:138–45.
45. Barad M, Gean P-W, Lutz B. The role of the amygdala in the extinction of conditioned fear. Biol Psychiat. 2006;60(4):322–8.
46. Adolphs R, Tranel D, Damasio H, Damasio A. Impaired recognition of emotion in facial expressions following bilateral damage to the human amygdala. Nature. 1994. https://doi.org/10.1038/372669a0.
47. Rice K, Viscomi B, Riggins T, Redcay E. Amygdala volume linked to individual differences in mental state inference in early childhood and adulthood. Dev Cogn Neurosci. 2014;8:153–63.

48. Nordahl CW, Scholz R, Yang X, Buonocore MH, Simon T, Rogers S, et al. Increased rate of amygdala growth in children aged 2 to 4 years with autism spectrum disorders: a longitudinal study. Arch Gen Psychiatry. 2012;69(1):53–61.
49. Herrington JD, Maddox BB, Kerns CM, Rump K, Worley JA, Bush JC, et al. Amygdala volume differences in autism spectrum disorder are related to anxiety. J Autism Dev Disord. 2017;47(12):3682–91.
50. Dalton KM, Nacewicz BM, Alexander AL, Davidson RJ. Gaze-fixation, brain activation, and amygdala volume in unaffected siblings of individuals with autism. Biol Psychiat. 2007;61(4):512–20.
51. Radeloff D, Ciaramidaro A, Siniatchkin M, Hainz D, Schlitt S, Weber B, et al. Structural alterations of the social brain: a comparison between schizophrenia and autism. PLoS ONE. 2014;9(9):e106539.
52. Lim L, Chantiluke K, Cubillo A, Smith A, Simmons A, Mehta M, et al. Disorder-specific grey matter deficits in attention deficit hyperactivity disorder relative to autism spectrum disorder. Psychol Med. 2015. https://doi.org/10.1017/S0033291714001974.
53. Stuss DT, Knight RT. Principles of frontal lobe function. Oxford: Oxford University Press; 2013.
54. Oades RD. Frontal, temporal and lateralized brain function in children with attention-deficit hyperactivity disorder: a psychophysiological and neuropsychological viewpoint on development. Behav Brain Res. 1998;94(1):83–95.
55. Balleine BW, Delgado MR, Hikosaka O. The role of the dorsal striatum in reward and decision-making. J Neurosci. 2007;27(31):8161–5.
56. Sato W, Kubota Y, Kochiyama T, Uono S, Yoshimura S, Sawada R, et al. Increased putamen volume in adults with autism spectrum disorder. Front Human Neurosci. 2014;8:957.
57. Estes A, Shaw DW, Sparks BF, Friedman S, Giedd JN, Dawson G, et al. Basal ganglia morphometry and repetitive behavior in young children with autism spectrum disorder. Autism Res. 2011;4(3):212–20.
58. Langen M, Schnack HG, Nederveen H, Bos D, Lahuis BE, de Jonge MV, et al. Changes in the developmental trajectories of striatum in autism. Biol Psychiatry. 2009;66(4):327–33.
59. Herbert M, Ziegler D, Deutsch C, O'brien L, Lange N, Bakardjiev A, et al. Dissociations of cerebral cortex, subcortical and cerebral white matter volumes in autistic boys. Brain. 2003;126(5):1182–92.
60. Bookheimer SY. Precentral Gyrus. In: Volkmar FR, editor. Encyclopedia of autism spectrum disorders. New York: Springer New York; 2013. p. 2334–5.
61. Sussman D, Leung R, Vogan V, Lee W, Trelle S, Lin S, et al. The autism puzzle: Diffuse but not pervasive neuroanatomical abnormalities in children with ASD. NeuroImage Clin. 2015. https://doi.org/10.1016/j.nicl.2015.04.008.
62. Tamura R, Kitamura H, Endo T, Hasegawa N, Someya T. Reduced thalamic volume observed across different subgroups of autism spectrum disorders. Psychiatry Res. 2010;184(3):186–8.
63. Tsatsanis KD, Rourke BP, Klin A, Volkmar FR, Cicchetti D, Schultz RT. Reduced thalamic volume in high-functioning individuals with autism. Biol Psychiat. 2003;53(2):121–9.
64. Lin H-Y, Ni H-C, Lai M-C, Tseng W-YI, Gau SS-F. Regional brain volume differences between males with and without autism spectrum disorder are highly age-dependent. Mol Autism. 2015;6(1):29.
65. Uppal N, Hof PR. Discrete cortical neuropathology in autism spectrum disorders. Neurosci Autism Spectrum Disord. 2013;313:325.
66. Kmccartney L, Bau K, Stewart K, Botha B, Morrow A. Pallidotomy as a treatment option for a complex patient with severe dystonia. Dev Med Child Neurol. 2016;58:68.
67. Turner AH, Greenspan KS, van Erp TG. Pallidum and lateral ventricle volume enlargement in autism spectrum disorder. Psychiatry Res. 2016;252:40–5.
68. Napier TC, Mickiewicz AL. The role of the ventral pallidum in psychiatric disorders. Neuropsychopharmacology. 2010;35(1):337.
69. Casanova MF, El-Baz A, Mott M, Mannheim G, Hassan H, Fahmi R, et al. Reduced gyral window and corpus callosum size in autism: possible macroscopic correlates of a minicolumnopathy. J Autism Dev Disord. 2009;39(5):751–64.
70. Freitag CM, Luders E, Hulst HE, Narr KL, Thompson PM, Toga AW, et al. Total brain volume and corpus callosum size in medication-naive adolescents and young adults with autism spectrum disorder. Biol Psychiatry. 2009;66(4):316–9.
71. Hardan AY, Pabalan M, Gupta N, Bansal R, Melhem NM, Fedorov S, et al. Corpus callosum volume in children with autism. Psychiatry Res. 2009;174(1):57–61.
72. Boger-Megiddo I, Shaw DW, Friedman SD, Sparks BF, Artru AA, Giedd JN, et al. Corpus callosum morphometrics in young children with autism spectrum disorder. J Autism Dev Disord. 2006;36(6):733–9.
73. Egaas B, Courchesne E, Saitoh O. Reduced size of corpus callosum in autism. Arch Neurol. 1995;52(8):794–801.
74. Hirosawa T, Kontani K, Fukai M, Kameya M, Soma D, Hino S, et al. Different associations between intelligence and social cognition in children with and without autism spectrum disorders. PLoS ONE. 2020;15(8):e0235380.
75. Haldane M, Cunningham G, Androutsos C, Frangou S. Structural brain correlates of response inhibition in Bipolar Disorder I. J Psychopharmacol. 2008;22(2):138–43.
76. Bogousslavsky J, Miklossy J, Deruaz J-P, Assal G, Regli F. Lingual and fusiform gyri in visual processing: a clinico-pathologic study of superior altitudinal hemianopia. J Neurol Neurosurg Psychiatry. 1987;50(5):607–14.
77. Michael C, Tranel D 2nd. Neuroscience in Medicine. Totowa: Humana Press; 2003.
78. Schremm A, Novén M, Horne M, Söderström P, van Westen D, Roll M. Cortical thickness of planum temporale and pars opercularis in native language tone processing. Brain Lang. 2018;176:42–7.
79. Blank SC, Scott SK, Murphy K, Warburton E, Wise RJ. Speech production: Wernicke. Broca Beyond Brain. 2002;125(8):1829–38.
80. De Fossé L, Hodge SM, Makris N, Kennedy DN, Caviness VS, McGrath L, et al. Language-association cortex asymmetry in autism and specific language impairment. Ann Neurol. 2004;56(6):757–66.
81. Brun L, Auzias G, Viellard M, Villeneuve N, Girard N, Poinso F, et al. Localized misfolding within Broca's area as a distinctive feature of autistic disorder. Biol Psychiatry Cogn Neurosci Neuroimaging. 2016;1(2):160–8.
82. Bigler ED, Mortensen S, Neeley ES, Ozonoff S, Krasny L, Johnson M, et al. Superior temporal gyrus, language function, and autism. Dev Neuropsychol. 2007;31(2):217–38.
83. Jou RJ, Minshew NJ, Keshavan MS, Vitale MP, Hardan AY. Enlarged right superior temporal gyrus in children and adolescents with autism. Brain Res. 2010;1360:205–12.
84. Libero LE, DeRamus TP, Lahti AC, Deshpande G, Kana RK. Multimodal neuroimaging based classification of autism spectrum disorder using anatomical, neurochemical, and white matter correlates. Cortex. 2015;66:46–59.
85. Libero LE, DeRamus TP, Deshpande HD, Kana RK. Surface-based morphometry of the cortical architecture of autism spectrum disorders: volume, thickness, area, and gyrification. Neuropsychologia. 2014;62:1–10.
86. Ferreira NF, Oliveira VD, Amaral L, Mendonça R, Lima SS. Analysis of parahippocampal gyrus in 115 patients with hippocampal sclerosis. Arq Neuropsiquiatr. 2003;61:707–11.
87. Jiao Y, Chen R, Ke X, Chu K, Lu Z, Herskovits EH. Predictive models of autism spectrum disorder based on brain regional cortical thickness. Neuroimage. 2010;50(2):589–99.
88. Auzias G, Viellard M, Takerkart S, Villeneuve N, Poinso F, Da Fonséca D, et al, editors. Brain structural underpinnings of autism spectrum disorder revealed by sulcus-based morphometry. IEEE-EMBS International Conference on Biomedical and Health Informatics (BHI); IEEE; 2014.
89. Auzias G, Viellard M, Takerkart S, Villeneuve N, Poinso F, Da Fonséca D, et al. Atypical sulcal anatomy in young children with autism spectrum disorder. NeuroImage Clin. 2014;4:593–603.
90. Pelphrey KA, Carter EJ. Brain mechanisms for social perception: lessons from autism and typical development. Ann N Y Acad Sci. 2008;1145:283.
91. Ecker C, Ronan L, Feng Y, Daly E, Murphy C, Ginestet CE, et al. Intrinsic gray-matter connectivity of the brain in adults with autism spectrum disorder. Proc Natl Acad Sci. 2013;110(32):13222–7.
92. Pappaianni E, Siugzdaite R, Vettori S, Venuti P, Job R, Grecucci A. Three shades of grey: detecting brain abnormalities in children with autism using source-, voxel-and surface-based morphometry. Eur J Neurosci. 2018;47(6):690–700.
93. Williams EL, El-Baz A, Nitzken M, Switala AE, Casanova MF. Spherical harmonic analysis of cortical complexity in autism and dyslexia. Transl Neurosci. 2012;3(1):36–40.

94. Yang DY-J, Beam D, Pelphrey KA, Abdullahi S, Jou RJ. Cortical morphological markers in children with autism: a structural magnetic resonance imaging study of thickness, area, volume, and gyrification. Mol Autism. 2016;7(1):11.
95. Maddock RJ, Garrett AS, Buonocore MH. Remembering familiar people: the posterior cingulate cortex and autobiographical memory retrieval. Neuroscience. 2001;104(3):667–76.
96. Maddock RJ, Garrett AS, Buonocore MH. Posterior cingulate cortex activation by emotional words: fMRI evidence from a valence decision task. Hum Brain Mapp. 2003;18(1):30–41.
97. Leech R, Sharp DJ. The role of the posterior cingulate cortex in cognition and disease. Brain. 2014;137(1):12–32.
98. Burstein R, Noseda R, Borsook D. Migraine: multiple processes, complex pathophysiology. J Neurosci. 2015;35(17):6619–29.
99. Tsao A, Sugar J, Lu L, Wang C, Knierim JJ, Moser M-B, et al. Integrating time from experience in the lateral entorhinal cortex. Nature. 2018;561(7721):57–62.
100. Demetriou EA, DeMayo MM, Guastella AJ. Executive function in autism spectrum disorder: history, theoretical models, empirical findings, and potential as an endophenotype. Front Psych. 2019;11(10):753.
101. Thabault M, Turpin V, Maisterrena A, Jaber M, Egloff M, Galvan L. Cerebellar and striatal implications in autism spectrum disorders: from clinical observations to animal models. Int J Mol Sci. 2022;23(4):2294.

Publisher's Note